

AN OPTIMIZED DIGITAL FILTER FOR THE COSINE TRANSFORM

Luiz Rijo

Universidade Federal do Pará - Departamento de Geofísica
C.P. 1611, Belém, PA, CEP: 66059-000, Brasil

Sine and cosine transforms are very important in electrical and electromagnetic methods. They are used, for instance, for computing two-dimensional Green functions in layered-earth models and for transforming electromagnetic responses from frequency to time domains. Currently, the best way to compute sine and cosine transforms in electrical geophysics is to employ the digital linear filter algorithm. Until recently, these filters had an excessive number of coefficients, which was a drawback for many applications. Recently, an optimized digital filter for sine transform with only 20 coefficients has appeared in the literature. In many applications the cosine transform is as important as the sine transform, so, we present here an optimized digital filter for the cosine transform, which has only 19 coefficients. Like the sine transform filter, it was generated by the Wiener-Hopf minimization process via Guptasarma trial and error strategy. Its performance has been exhaustively tested. It always yields good results, as the examples illustrated in this paper.

UM FILTRO DIGITAL OTIMIZADO PARA A TRANSFORMADA CO-SENO *As transformadas seno e co-seno são muito importantes nos métodos elétricos e eletromagnéticos. Elas são usadas, por exemplo, para calcular funções de Green bidimensionais de meios estratificados e para transformar respostas eletromagnéticas do domínio da frequência para o domínio do tempo. Atualmente, a melhor maneira de computar transformadas seno e co-seno, nos métodos elétricos e eletromagnéticos, é através do algoritmo dos filtros lineares digitais. Até recentemente, esses filtros continham um número excessivo de coeficientes, o que constituía uma grande desvantagem em muitas aplicações. Recentemente, um filtro otimizado, para transformada seno, com apenas 20 coeficientes, foi publicado na literatura. Considerando que em muitas aplicações a transformada co-seno é tão importante quanto a transformada seno, apresentamos, neste trabalho, um filtro linear otimizado com apenas 19 coeficientes para essa transformada. A exemplo do filtro para a transformada seno, este também foi obtido através do método dos mínimos quadráticos de Wiener-Hopf junto com o esquema de otimização de Guptasarma. Ele foi exaustivamente testado, apresentando sempre bons resultados, como mostram os exemplos ilustrados neste artigo.*

INTRODUCTION

Fourier and Hankel transforms are widely used in electrical and electromagnetic methods. Their numerical computations were extremely troublesome before the introduction of the digital linear filter algorithm by Ghosh in 1971. Since then, there has been a continuous progress toward better algorithms (Koefoed et al., 1972; Das and Ghosh 1974; Verma, 1977; Koefoed and Dirks, 1979; Johansen and Sorensen, 1979; Anderson, 1979; Guptasarma, 1982; Nissen and Enmark, 1986, O'Neill, 1975; Verma and Koefoed, 1973).

The digital linear filter algorithm is based on the transformation of the Fourier (or Hankel) transform into a convolution integral (Kunetz, 1966). The fundamental contribution by Ghosh (1971) was to devise a simple scheme, based on sampling theory, for computing numerically such convolution through digital linear filter. Meanwhile, in 1979, Koefoed and Dirks proposed a new scheme, based on the Wiener-Hopf least-squared technique, for designing linear filter for the Hankel transform in a much easier and more efficient manner than that used by Ghosh. In 1982, Guptasarma implemented a strategy to improve the method of Koefoed and Dirks and gave some short, optimized filter for Hankel transform.

Using Guptasarma scheme, Nissen and Enmark (1986) constructed an optimized short filter for the sine transform with only 20 coefficients. Moreover, they suggested that the cosine transform

$$F(x) = \int_0^{\infty} f(k_x) \cos(k_x x) dk_x, \quad (1)$$

be rewritten in the form

$$F(x) = \frac{-1}{x} \int_0^{\infty} f'(k_x) \sin(k_x x) dk_x, \quad (2)$$

and that the sine transform digital filter be subse-

quently applied. For this reason, they published only the filter for the sine transform.

Unfortunately, in the most important problems in the electrical and electromagnetic methods, the Kernel function $f(k_x)$ in (1) is known only at very few discrete points. Therefore it is not practical to use (2), due to the difficulties in handling numerical derivatives of a discrete function. For this reason, it is important to have, also, digital linear filters for the cosine transform.

In 1979, Anderson reported two digital linear filters for the sine and cosine transforms computed by the Ghosh methods. Despite their high precision, they have too many coefficients, which are an enormous hindrance for cosine transforming of Kernel functions generated by costly numerical algorithms like finite elements and integral equation. This happens, for instance, when transforming EM data of 2D and 3D models from frequency to time domains.

The aim of this paper is to present an optimized digital linear filter for the cosine transform with a small number of coefficients. It was calculated by the Wiener-Hopf least-squared technique with Guptasarma strategy like Nissen and Enmark sine transform filter.

THE DIGITAL FILTER FOR THE COSINE TRANSFORM

With a simple transformation of variables, the integral (1) can be replaced by

$$xF(x) = \int_0^{\infty} f(k_x/x) \cos(k_x) dk_x. \quad (3)$$

Now, substituting x for e^p and k_x for e^s we obtain the convolution integral

$$xF(x) = \int_{-\infty}^{\infty} f(e^{-(p-s)}) e^s \cos(e^s) ds, \quad (4)$$

where $f(e^{-(p-s)})$ and $xF(x)$ are, respectively, the input and output functions and $e^s \cos(e^s)$ the *filter function*. Following Guptasarma (1982), our objec-

tive is to approximate the integral (4) by the discrete convolution,

$${}_x F(x) = \sum_{n=1}^N f(e^{-(nx - (a_1 + (n-1)T))}) W_n + \epsilon, \quad (5)$$

where ϵ is the error due to the discrete approximation. To obtain the filter coefficients W_n we used the Wiener-Hopf least-squared method described by Koefoed and Dirks (1979), improved by the trial and error scheme proposed by Guptasarma (1982). The details are not given here because they are well-explained in the original papers.

To construct the filter we have used the following functions

$$f(k_x) = k_x^2 e^{-ak_x} \quad (6)$$

and

$${}_x F(x) = \frac{2a(a^2 - 3x^2)}{(a^2 + x^2)^3}, \quad (7)$$

and for monitoring the error in the Guptasarma scheme, we applied the expression

$$\int_0^\infty e^{-a^2 k_x^2} \cos(k_x x) dk_x = \frac{\sqrt{\pi}}{2a} e^{-x^2/4a^2}, \quad (8)$$

resulting in $a_1 = 6.0$ for the first abscissa and $T = 0.48$ for the abscissa increment. With these values for a_1 and T in (5), the Wiener-Hopf least-squared criterion generates the filter coefficients shown in Table 1.

APPLICATION OF THE FILTER

To illustrate the performance of the filter given in Table 1 we selected six typical examples of cosine transforms frequently found in electrical geophysics.

Electrical field in frequency domain on a half-space

Table 1. Abscissas and coefficients of the filter.

No.	Abcissas	Coefficients W_n
1	-6.00	0.6213729E - 02
2	-5.52	-0.7106100E - 02
3	-5.04	0.1392100E - 01
4	-4.56	-0.5513420E - 02
5	-4.08	0.1738963E - 01
6	-3.60	0.5178800E - 02
7	-3.12	0.2820408E - 01
8	-2.64	0.2730540E - 01
9	-2.16	0.6264861E - 01
10	-1.68	0.7816871E - 01
11	-1.20	0.1516985E + 00
12	-0.72	0.1862742E + 00
13	-0.24	0.2976519E + 00
14	0.24	0.1323330E + 00
15	0.72	-0.3889732E + 00
16	1.20	-0.1640198E + 01
17	1.68	0.1373593E + 01
18	2.16	-0.3914654E + 00
19	2.64	0.5267562E - 01

Our first example deals with the electrical field of an infinite line-source of current ($I=2A$) oriented in the y -direction on the surface of a conductive half-space. Using the quasi-static approximation, the field, in the frequency domain, is expressed by (Ward & Hohmann, 1988)

$$E_y(x, 0, \omega) = \frac{-i\omega\mu_0 I}{\pi} \int_0^\infty \frac{1}{k_x + u} \cos(k_x x) dk_x, \quad (9)$$

where $u = (k_x^2 + i\omega\mu_0\sigma)^{1/2}$ is the propagation constant in the half-space, $\mu_0 = 4\pi 10^{-7} H/m$ the vacuum permeability and $\omega = 2\pi f$ the current angular frequency. In this particular case, the integral (9) has the equivalent closed form expression

$$E_y(x, 0, \omega) = \frac{-i\omega\mu_0 I}{\pi k^2 x^2} [1 - ikx K_1(ikx)], \quad (10)$$

where K_1 is the modified Bessel function of first order and second kind and $k^2 = -i\omega\mu_0\sigma$ is the wave-number of the half-space (Ward & Hohmann, 1988). Fig. 1 shows the electrical field response versus frequency, at 100 m from the line-source on a 10 Ωm

half-space, computed using (5) with the 19 coefficient filter, compared to the exact solution (10). Table 2 shows the corresponding numerical values. The agreement is very good.

Electrical field in time domain on a half-space

Using the previous model, let us calculate the transient response due to a negative step current. This can be accomplished by performing the inverse Fourier transform of (9). Exploring the symmetry properties of the Fourier transform (Papoulis, 1962) we can write

$$A = \left[\int_0^\infty \frac{i}{k_x + u} \cos(k_x x) dk_x \right]$$

$$e_y(x, 0, t) = \frac{2\mu_0 I}{\pi^2} \int_0^\infty \Im A \cos(\omega t) d\omega. \quad (11)$$

Note that we have now two independent cosine transforms. Therefore, we need to use the digital filter twice. This process can be carried out efficiently by exploring the convolution properties of (5). As in the previous case, the expression (11) has an equivalent closed form given by

$$e_y(x, 0, t) = \frac{I}{\pi \sigma x^2} (1 - e^{-\theta^2 x^2}), \quad (12)$$

where $\theta = (\sigma \mu_0 / 4t)^{1/2}$. It is important to emphasize that, in general, closed form expressions are not always available. Usually the field is expressed in integral form. Thus, having efficient numerical integration algorithms is always necessary. Fig. 2 compares the results using the 19 filter convolution and the exact solution. The agreement is also perfect.

Electrical field in time domain within a half-space

Computation of electrical fields within a layered-earth host is a necessary step toward the finite element method calculation of electrical fields due to two-dimensional inhomogeneities. Thus, our next example is to compute the transient electrical fields

within a half-space due to a line of current on the surface. The negative step response at a point (x, z) within the earth is given by

$$A = \left[\int_0^\infty \frac{i e^{u^2}}{k_x + u} \cos(k_x x) dk_x \right]$$

$$e_y(x, 0, t) = \frac{2\mu_0 I}{\pi^2} \int_0^\infty \Im A \cos(\omega t) d\omega, \quad (13)$$

which is equivalent to (Oristaglio, 1982)

$$A = 2\theta^2 z^2 e^{-\theta^2 r^2}$$

$$B = \frac{x^2 - z^2}{r^2} \left[\operatorname{erfc}(\theta z) - e^{-\theta^2 r^2} \right]$$

$$C = -\frac{2\theta z}{\sqrt{\pi}} e^{-\theta^2 z^2}$$

$$D = \left[1 - 2\theta x \left(1 + \frac{1}{\theta^2 r^2} \right) \mathcal{F}(\theta x) \right]$$

$$e_y(x, 0, t) = \frac{I}{\pi \sigma r^2} \{A + B - C(D)\}, \quad (14)$$

where $\theta = \sigma \mu_0 / 4t$. The functions $\operatorname{erfc}(x)$ and $\mathcal{F}(x)$ are, respectively, the complementary error function and the Dawson function. Fig. 3 shows the transient electrical field at the depth of 120 m and 85 m from the line within a 100 Ωm half-space, computed using (13) with the 19 filter convolution and the field calculated from the closed form (14). The agreement is excellent.

Two-dimensional Green function of a two-layered earth

In the first example, the line and the observation point were both on the surface. In the second, the observation point was located within the earth, whereas the line was maintained on the surface. Now, let us locate both of them below the surface as shown in Fig. 4. This is known as two-dimensional Green function problem and it is commonly used in 2-D integral equation modelling.

The Green function $G(x, y; x', y')$ at the second layer of a two-layered earth, with the quasi-static approximation, is expressed by

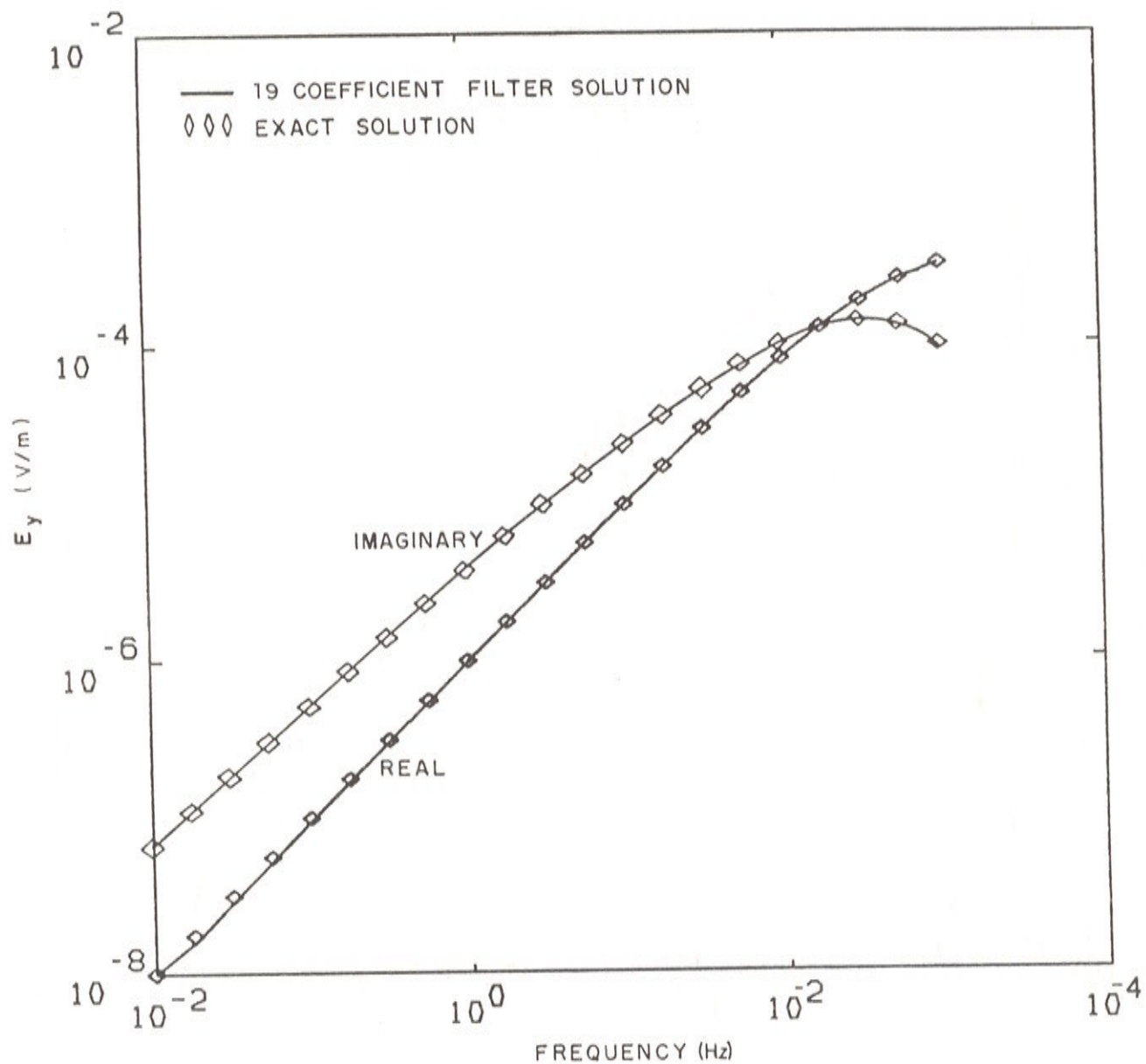


Figure 1. Exact and numerical solutions of the electrical field, in the frequency domain, at 100 m from a line source on a 10Ω m half-space.

Soluções exata e aproximada do campo elétrico, no domínio da frequência, a 100 m de uma linha de corrente (1 A) na superfície de um semi-espaco de 10Ω m.

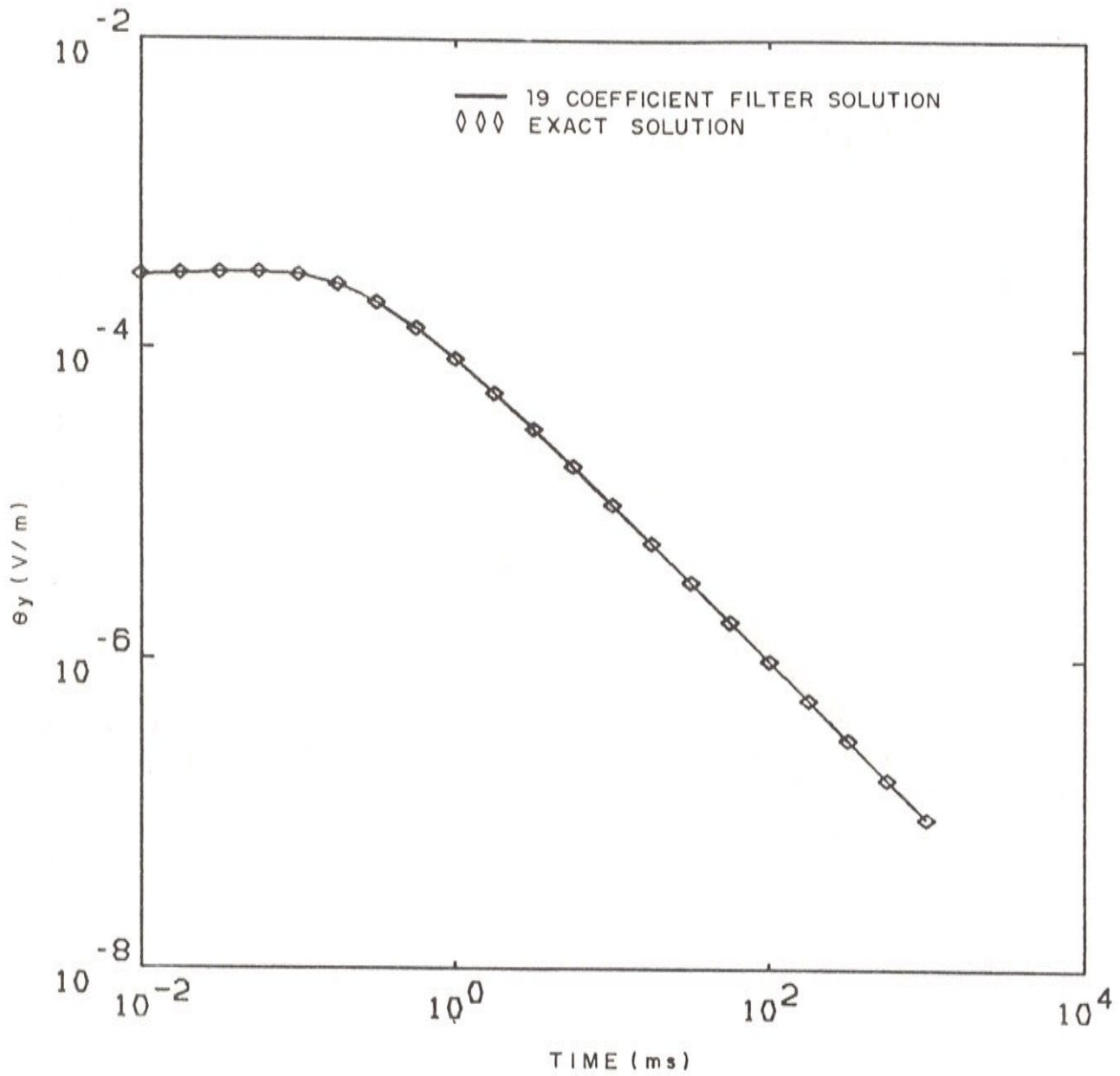


Figure 2. Exact and numerical solutions of the transient electrical field at 100 m from a line source on a 10Ω m half-space.

Soluções exata e aproximada do campo elétrico transiente a 100 m de uma linha de corrente (1 A) na superfície de um semi-espaco de 10Ω m.

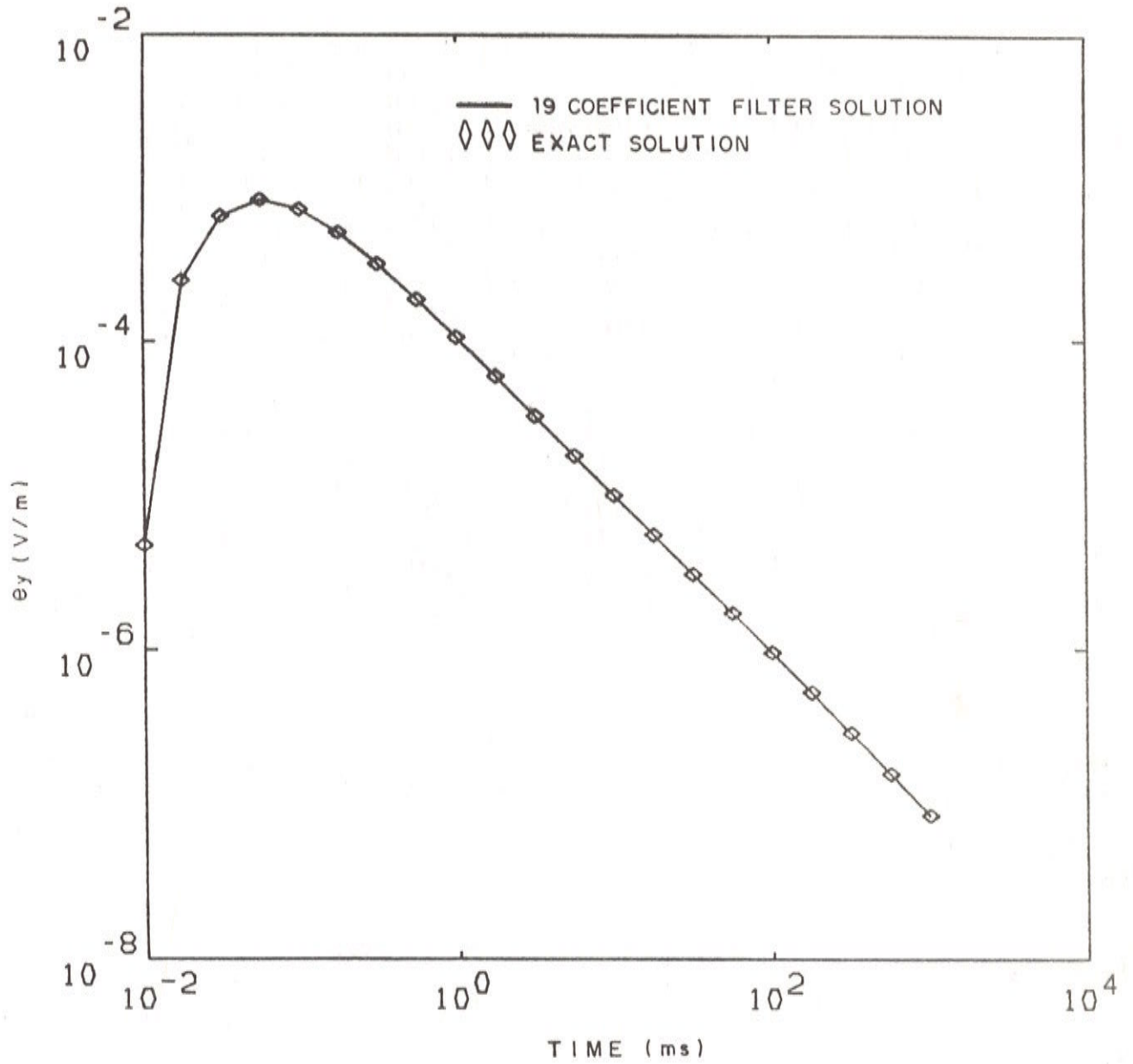


Figure 3. Exact and numerical solutions of the transient electrical field at 120 m from a line source and at the depth of 85 m in a $10 \Omega \text{ m}$ half-space.

Soluções exata e aproximada do campo elétrico transiente a 120 m de uma linha de corrente (1 A) e a 85 m de profundidade num semi-espaço de $10 \Omega \text{ m}$.

Table 2. Numerical values of the electrical field $E_y(x, 0, \omega)$

Freq. (Hz)	Numerical (V/m)		Exact (V/m)	
	Real	Imaginary	Real	Imaginary
0.0100	-0.8583E-08	-0.6585E-07	-0.9869E-08	-0.6709E-07
0.0178	-0.1587E-07	-0.1111E-06	-0.1755E-08	-0.1129E-06
0.0316	-0.2881E-07	-0.1869E-06	-0.3120E-07	-0.1893E-06
0.0562	-0.5233E-07	-0.3133E-06	-0.5548E-07	-0.3163E-06
0.1000	-0.9462E-07	-0.5222E-06	-0.9863E-07	-0.5263E-06
0.1778	-0.1698E-06	-0.8660E-06	-0.1753E-06	-0.8716E-06
0.3162	-0.3041E-06	-0.1428E-05	-0.3116E-06	-0.1436E-05
0.5623	-0.5438E-06	-0.2340E-05	-0.5534E-06	-0.2350E-05
1.0000	-0.9692E-06	-0.3804E-05	-0.9823E-06	-0.3817E-05
1.7783	-0.1724E-05	-0.6129E-05	-0.1741E-05	-0.6146E-05
3.1623	-0.3059E-05	-0.9766E-05	-0.3081E-05	-0.9789E-05
5.6234	-0.5404E-05	-0.1536E-04	-0.5435E-05	-0.1539E-04
10.0000	-0.9500E-05	-0.2375E-04	-0.9542E-05	-0.2379E-04
17.7828	-0.1658E-04	-0.3595E-04	-0.1663E-04	-0.3600E-04
31.6228	-0.2857E-04	-0.5291E-04	-0.2865E-04	-0.5299E-04
56.2341	-0.4839E-04	-0.7504E-04	-0.4850E-04	-0.7513E-04
100.0000	-0.7986E-04	-0.1011E-03	-0.7998E-04	-0.1012E-03
177.8279	-0.1268E-03	-0.1266E-03	-0.1269E-03	-0.1268E-03
316.2278	-0.1901E-03	-0.1425E-03	-0.1904E-03	-0.1428E-03
562.3413	-0.2635E-03	-0.1364E-03	-0.2638E-03	-0.1366E-03
1000.0000	-0.3280E-03	-0.9960E-04	-0.3282E-03	-0.9998E-04

$$G(x, y; x', y') = \frac{-1}{2\pi} \int_0^\infty \left[e^{u_2|z-z'|} + R_{TE} e^{-u_2(z+z')} \right] \frac{1}{u_2} \cos[k_x(x-x')] dk_x \quad (15)$$

where

$$R_{TE} = \left[\frac{(u_2 - u_1)(u_1 + u_x) + (u_2 + u_1)(u_1 - u_x)}{(u_2 + u_1)(u_1 + u_x) + (u_2 - u_1)(u_1 - u_x)} \right] e^{2u_2 d}, \quad (16)$$

is the reflection coefficients and $u_j = (k_x - i\omega\mu_0\sigma)^{1/2}$ is the propagation constant in the layers $j=1,2$ (Rijo, 1990). Fig. 5 shows the real and imaginary parts of the 2-D Green function computed with our short filter and Anderson's filter (1975).

Influence of the Gaussian electrojet on the MT response

The electrical and magnetic fields on the surface of an homogeneous earth subjected to a Gaussian electrojet are easily simulated by the convolution

of a line-source response with a planar Gaussian distribution of current, $I(x_0) = e^{-x_0^2/2s^2}$ (Peltier and Hermance, 1971; Mota and Rijo, 1991). After performing that convolution, the components of the field are

$$E_y(x, 0, \omega) = \frac{-i\omega\mu_0\sqrt{2}}{s\sqrt{\pi}} \int_0^\infty \left[\frac{e^{k_x h_0}}{k_x + u} e^{-k_x^2 s^2/2} \right] \cos(k_x x) dk_x \quad (17)$$

and

$$H_x(x, 0, \omega) = \frac{\sqrt{2}}{s\sqrt{\pi}} \int_0^\infty \left[u \frac{e^{k_x h_0}}{k_x + u} e^{-k_x^2 s^2/2} \right] \cos(k_x x) dk_x, \quad (18)$$

where h_0 is the height of the Gaussian electrojet and s its standard deviation. We used these expressions for computing the surface impedance $Z = -E_y/H_x$ and subsequently the magnetotelluric apparent resistivity.

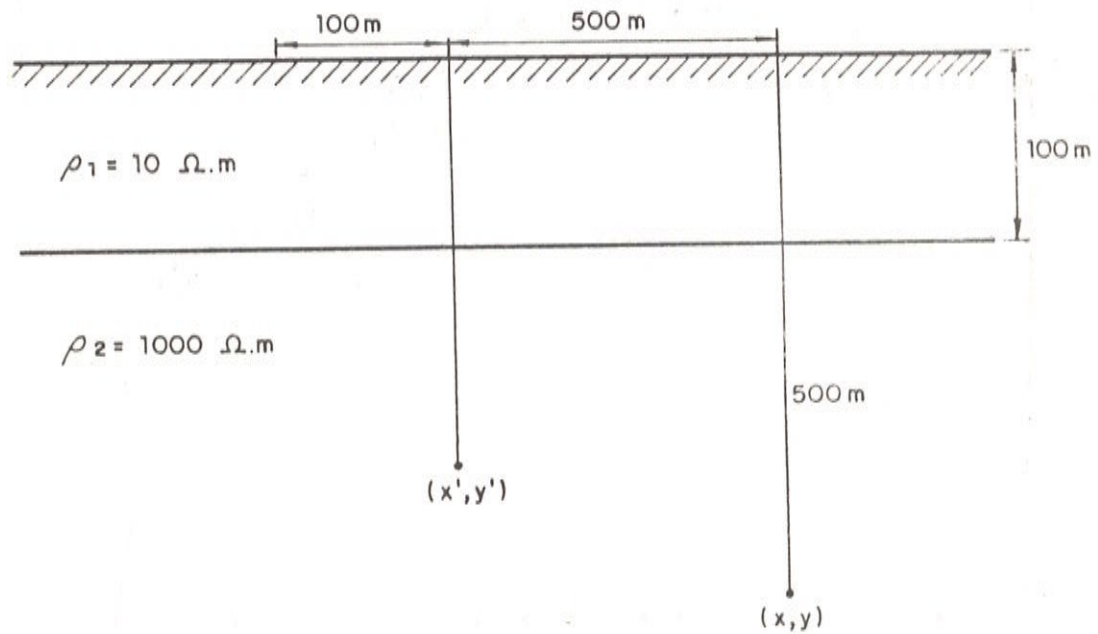


Figure 4. Geometry of the model for the 2-D Green function calculation.
Geometria do modelo para o cálculo da função de Green bidimensional.

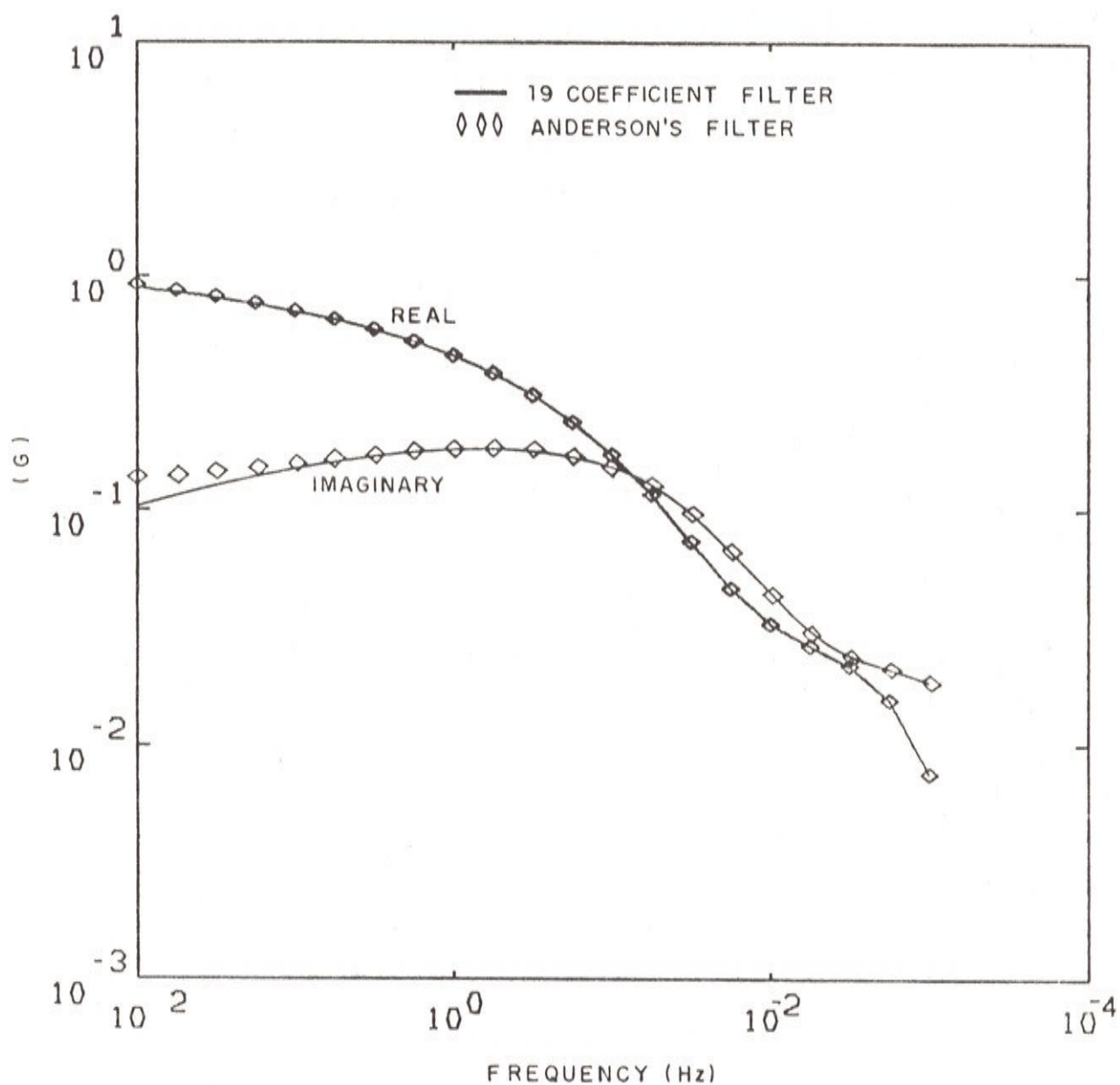


Figure 5. 2-D Green function calculated with the 19 coefficient filter and with Anderson's filter (1975).

Função de Green 2-D do modelo da Figura 4 computada com os filtros de 19 coeficientes e de Anderson (1975).

$$\rho_a = \frac{1}{\omega\mu_0} |Z|^2. \quad (19)$$

The curves of apparent resistivity and phase of the impedance due to an 10 Ωm homogeneous earth energized by a Gaussian electrojet, with standard deviation $s = 240$ km located at $h_0 = 110$ km above the surface, are illustrated in Fig. 6. These curves were computed with our short filter and with Anderson's filter.

Transient response of a complex model

The examples discussed so far do not show the actual advantage of employing a short filter for performing the cosine transform. The real benefit appears when we need to model a complex earth by numerical techniques, such as finite elements and integral equation. Most of the CPU time used by the integral equation algorithm is due to the enormous quantity of Green function computations. Therefore, it is crucial to have an efficient algorithm for cosine transform to implement cost-effective 2-D integral equation modelling. Another important situation, commonly found in practice is the calculation of transient responses of complex earth models. It is well-known (Papoulis, 1962) that the time domain response is given by the cosine transform,

$$e_y(x, 0, t) = \frac{-2}{\pi} \int_0^{\infty} \frac{\Im[E_y(x, 0, \omega)]}{\omega} \cos(\omega t) d\omega, \quad (20)$$

where the electrical field E_y in the frequency domain is computed by finite element or integral equation techniques, which demand a large amount of computer time. The transient response shown in Fig. 7 (Brochado, 1990) were computed using 19 frequency domain finite element solutions against 97 solutions with Anderson's filter.

CONCLUSION

Discrete sine and cosine transforms are fundamental tools in electrical geophysics. Nissen and Enmark(1986) used Guptasarma strategy to construct

an optimized digital filter for the sine transform which has proved very useful. Because a similar filter for the cosine transform was not available, we decided to design one having the same characteristics of the sine transform. To accomplish this, we also used Guptasarma scheme, which resulted in an optimized linear digital filter with 19 coefficients. As the examples given here show, the filter performs in a very satisfactory way. Short linear digital filters are very important in the pre and post-processing phases of numerical modelling, as for instance, 2-D Green function computations and transformation of EM responses from frequency to time domains. However, the most important application of a short filter is for synthesizing two-dimensional spectral solutions computed numerically by the finite element or integral equation methods to restore the final 2D-3D (two-dimensional earth with three dimensional source) solution (Rijo, 1990).

ACKNOWLEDGMENT

The research for this paper was supported by CNPq (Brazilian National Council for Science and Technology) and GTZ (Deutsche Gesellschaft für Technische Zusammenarbeit). We also thank Prof. Verma for his constructive comments.

REFERENCES

- ANDERSON, W.L. (1975) Improved digital filter for evaluating Fourier and Hankel transform integrals. NTIS PB-242 800, U.S. Department of Commerce.
- ANDERSON, W.L. (1979) Numerical integration of related Hankel transform of order 0 and 1 by adaptive digital filtering. *Geophysics*, **44**: 1287-1305.
- BROCHADO, S. (1990) Efeitos da topografia nos dados eletromagnéticos bidimensionais no do-

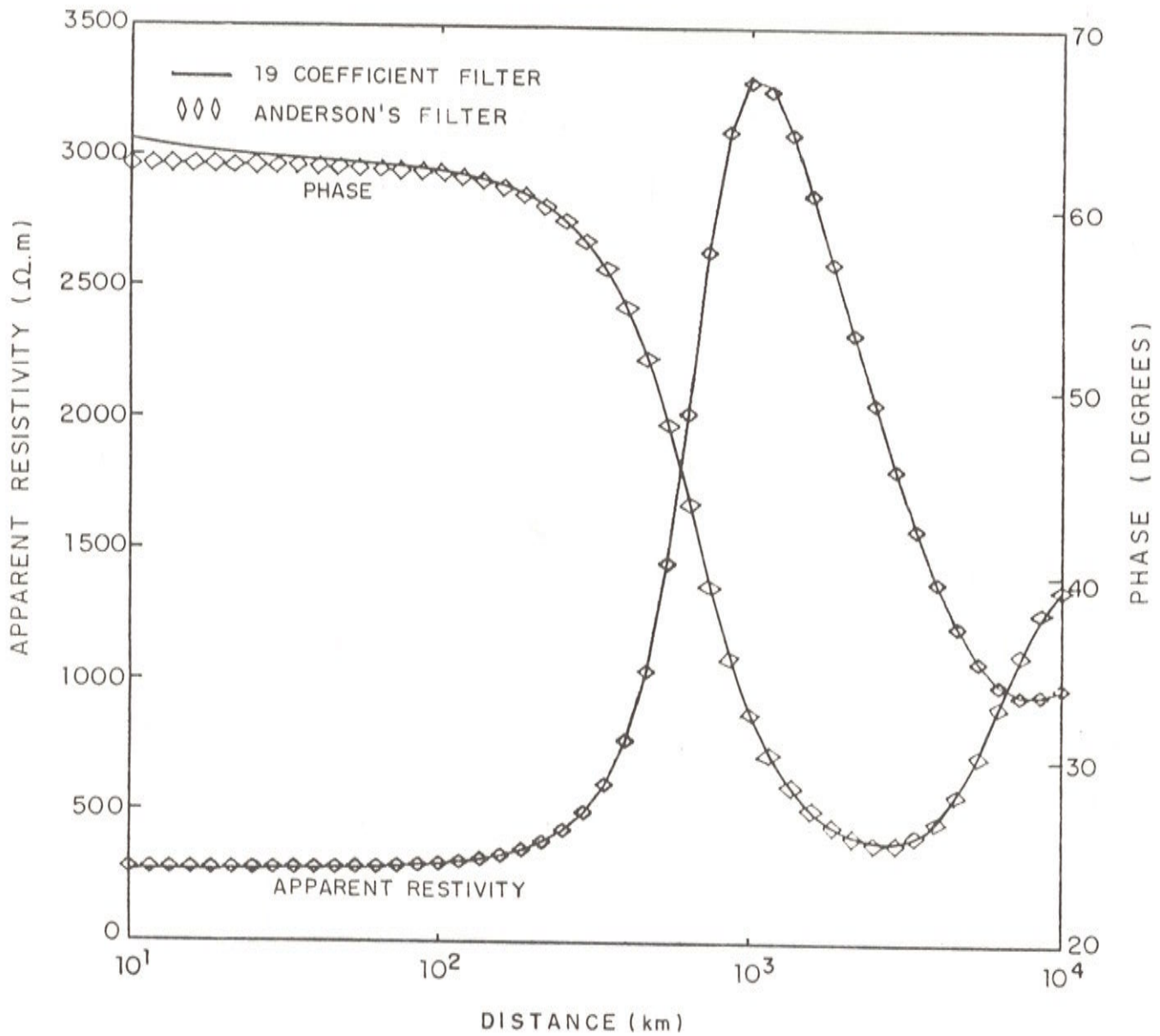


Figure 6. Magnetotelluric apparent resistivity and phase due to a $100 \Omega m$ half-space under a Gaussian electrode computed with the 19 coefficient filter and Anderson's filter (1975).

Resistividade aparente e fase MT devido a um semi-espaço de resistividade $100 \Omega m$ sobre a influência do electrojato gaussiano computado com os filtros de 19 coeficientes e de Anderson (1975).

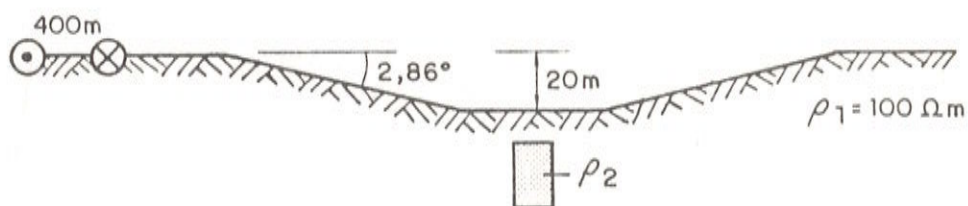
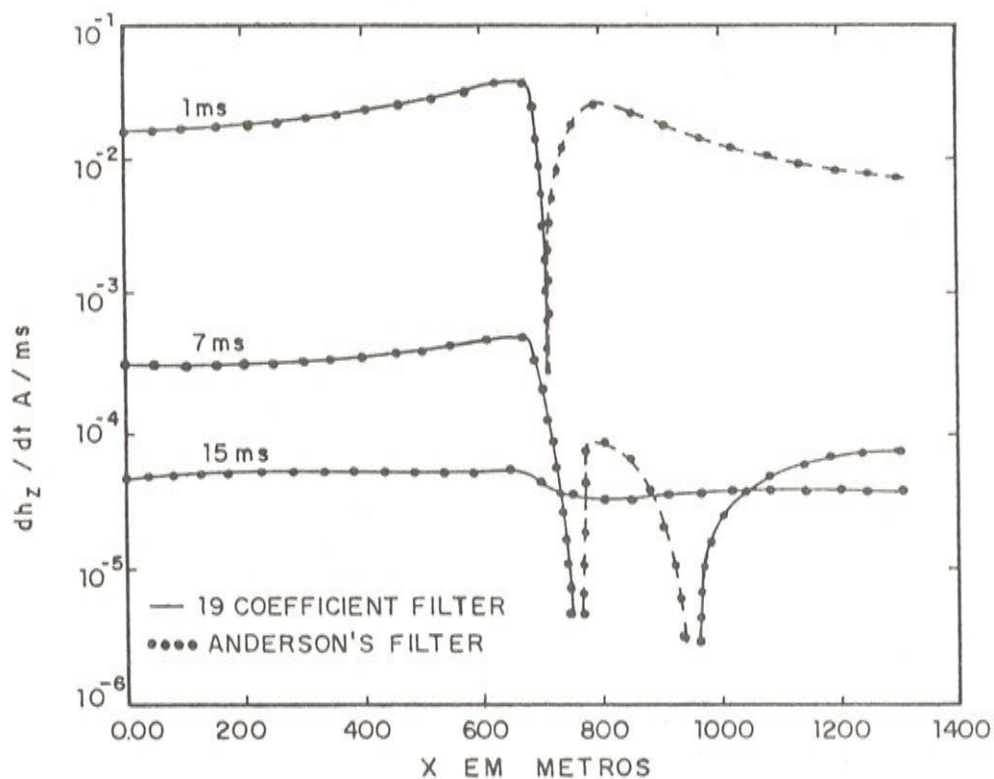


Figure 7. Transient response of a dike in a topographic terrain, energized with two infinite lines of current computed with the 19 coefficient filter and Anderson's filter (1975) (Brochado, 1990), (Solid line: positive-response, dashed line: negative-response).

Resposta transiente de um dique na presença de topografia, energizado por duas linhas de corrente computadas com os filtros de 19 coeficientes e de Anderson (1975) (Brochado 1990), (Linha cheia: resposta-positiva; linha tracejada: resposta-negativa).

- mínio do tempo e da frequência. Tese de Mestrado, CG/UFPa, 61 pp.
- DAS, U.C. and GHOSH, D.P.** (1974) The determination of filter coefficients for computation of standard curves for dipole resistivity sounding over layered earth by linear digital filter. *Geophysical Prospecting*, **22**: 765-780.
- GHOSH, D.P.** (1971) The application of linear filter theory to the direct interpretation of geoelectrical resistivity sounding measurements. *Geophysical Prospecting*, **30**: 501-514.
- GUPTASARMA, D.** (1982) Optimization of short digital linear filters for increased accuracy. *Geophysical Prospecting*, **30**:501- 514.
- JOHANSEN, H.K. and SØRENSEN, K.** (1979) Fast Hankel transforms. *Geophysical Prospecting*, **27**: 876-901.
- KOEFOED, O., GHOSH, D.P. and POLMAN, G.J.** (1972) Computation of type curves for electromagnetic depth sounding with a horizontal transmitting coil by means of a digital linear filter. *Geophysical Prospecting*, **20**: 407-420.
- KOEFOED, O. and DIRKS, F.J.H.** (1979) Determination of resistivity sounding filter by the Wiener-Hopf least-squared method. *Geophysical Prospecting*, **27**: 245-250.
- KUNETZ, G.** (1966) Principles of direct current resistivity prospecting. Gebrüder Borntraeger, Berlim, 103 pp.
- MOTA, J.P. and RIJO, L.** (1991) Efeitos do eletrojato equatorial na resistividade aparente e fase no método magnetotelúrico. *Revista Brasileira de Geofísica*, **9**: 161-177.
- NISSEN, J. and ENMARK, T.** (1986) An optimized digital filter for the Fourier transform. *Geophysical Prospecting*, **34**: 897-903.
- O'NEILL, D.J.** (1975) Improved linear filter coefficients for application in apparent resistivity amputations. *Bull. Australian SEG*, **6**: 104-109.
- ORISTAGLIO, A.** (1982) Diffusion of electromagnetic fields into the earth from line source of current. *Geophysics*, **47**: 1585- 1592.
- PAPOULIS, A.** (1962) The Fourier integral and its applications. McGraw-Hill Book Comp., N.Y. 318 pp.
- PELTIER, W. and HERMANCE, J.F.** (1971) Magnetotelluric fields of a Gaussian electrojet. *Can. J. of Earth Sci.*, **8**: 338-346.
- RIJO, L.** (1990) Teoria dos Métodos Eletromagnéticos. Notas de Aulas-Belém(PA), UFPa, 271 pp.
- VERMA, R. K. and KOEFOED, O.** (1973) Anote on the linear filter method of computing electromagnetic sounding curves. *Geophysical Prospecting*, **21**: 70-76.
- VERMA, R.K.** (1977) Detectability by electromagnetic sounding system. *IEEE Trans. Geosci. Electr.*, **GE-15**: 232-251.
- WARD, S.H. and HOHMANN, G.W.** (1988) Electromagnetic theory for geophysical applications in "Electromagnetic Methods in Applied Geophysics" Edited by Nabighian, M.N., Investigations in Geophysics No.3, SEG, Tulsa.

Submetido em: 02-07-91

Revisado em: 25-02-93

Aceito em: 25-02-93

Editor associado: Wladimir Shukowsky